SUPPLEMENTARY INFORMATION

1 Pulsation Analysis

Light curves for all stars were downloaded from MAST (Barbara A. Mikulski Archive for Space Telescopes)[1]. We used the Pre-search Data Conditioning Simple Aperture Photometry (PDCSAP) to calculate the Fourier amplitude spectra. To rule out contamination from blends as the source of the δ Scuti pulsations we examined *TESS* pixel data and cross-matched with the Gaia DR2 catalogue. We were able to rule out contamination within 21 arcsec (~ 1 TESS pixel) down to a magnitude difference of 9 in *Gaia* G band, except for four targets that appear to be resolved binaries in the *Gaia* DR2 catalogue.

The large separation $\Delta\nu$ for each star is listed in Table S1. In most cases this was measured by aligning the highest-frequency radial modes in a vertical ridge in the échelle diagram (see Fig. 1). In stars without a clear sequence of radial modes, such as those in Fig. 4, $\Delta\nu$ was similarly chosen to make the ridges vertical but is less well constrained because there are several ridges that are not quite parallel.

The phase term ϵ is given for those stars having a clear $l = 0$ sequence, as determined from the horizontal position of that ridge in the échelle diagram. Note that $\Delta\nu$ and ϵ are related to the frequencies of high-order radial modes via the asymptotic relation: $\nu_{n,l=0} \approx \Delta\nu(n + \epsilon)$.

2 Fundamental Stellar Properties

To estimate properties for our sample we used Tycho B_T and V_T photometry[2], which we transformed into Johnson B and V magnitudes[3]. We then used a $(B - V)$–$T_{\rm eff}$ relation[4], Gaia DR2 parallaxes[5], a 3D dust map[6], and V-band bolometric corrections to calculate effective temperatures and luminosities. We did this by solving for the distance modulus, as implemented in the "direct mode" version of `isoclassify`[7]. For stars with typical uncertainties > 0.01 mag in Tycho ($V_T > 9$ mag) we used Gaia $BP - RP$, with which we interpolated the colour–$T_{\rm eff}$ relation in the MIST (MESA Isochrones and Stellar Tracks) model grid[8] for solar metallicity to derive $T_{\rm eff}$, and used 2MASS K-band magnitudes in combination with Gaia parallaxes to derive luminosities.

We adopted 2% fractional uncertainties for all derived effective temperatures, which is typical of the residual scatter in optical colour-temperature relations[9]. A comparison of our Gaia-derived temperatures with those derived from Tycho photometry for stars with $V_T < 10$ mag, and a comparison with an independent implementation of the infrared flux method (IRFM), both showed good agreement with no significant systematic offsets. Our effective temperatures are on average $\sim 1.5\%$ ($\approx$ 200 K) hotter than those for A-type stars in the *Kepler* Stellar Properties Catalog[10,11], which were predominantly based on the Kepler Input Catalog (KIC)[12]. Such systematic differences are typical for effective temperature scales in A stars, reflecting the fact that the KIC was not optimized for A stars.

To estimate mean stellar densities, we fitted the effective temperatures and luminosities derived in the previous step to MIST isochrones using the "grid mode" of `isoclassify`, assuming a solar-neighborhood metallicity prior. The procedure also yielded estimates of stellar masses and surface gravities, which combined with $T_{\rm eff}$ were used for the interpolation of bolometric corrections in the previous step. We iterated between the "direct mode" and "grid mode" calculations

until all values were converged. Table S1 lists all stellar properties of the sample. Typical uncertainties are $\sim 3\,\%$ in luminosity and $\sim 12\,\%$ in mean stellar density. The properties of V1366 Ori (HD 34282) are not shown because they are highly uncertain due to obscuration by circumstellar material (it is classified as a Herbig Ae star)[13]. This star is not plotted in Fig. 3.

To identify close binaries, which could bias the derived stellar parameters, we cross-matched our targets with the Washington Double Star (WDS) catalog[14]. We also calculated the *Gaia* DR2 re-normalized unit weight error (RUWE) for each target, which provides a quality metric that accounts for the effects of colour and apparent magnitude on *Gaia* astrometric solutions. Stars with WDS companions within 2 arcsec or Gaia RUWE > 2 are marked with an asterisk in Table S1 and were not plotted in Fig. 3.

3 High-Resolution Spectroscopy

We obtained optical high-dispersion spectra of some stars in the sample in April and May 2019 using the HIRES spectrograph[15] at the Keck-I 10-m telescope on Maunakea observatory, Hawai'i. The spectra were obtained and reduced as part of the California Planet Search queue[16]. We typically obtained 1-minute integrations using the C5 decker, resulting in a S/N per pixel of 50 at ~ 600 nm with a spectral resolution of $R \sim 60000$.

High-resolution spectra for some stars were obtained in May and June 2019 using the NRES spectrograph[17] at the Las Cumbres Observatory Global Telescope Network[18] 1-meter telescopes at Cerro Tololo Inter-American Observatory, Chile and Sutherland (South Africa). Exposure times were typically 10 minutes, resulting in a S/N per resolution element above 70 at ~ 510 nm, with a spectral resolution of $R \sim 50000$.

Figure S2 shows a small region of each spectrum, alongside the Fourier amplitude spectrum. The spectral analysis was performed using the UCLSYN spectral synthesis package[19,20] using ATLAS9 models without convective overshooting[21]. Atomic data used in the analysis was obtained from the VALD database[22], using their default search and extraction parameters. Surface gravities were fixed to $\log g = 4.0$ for all stars in the analysis. A microturbulence value of 3 km s^{-1} was assumed, which is the typical value for stars within the spectral range considered here[23,24]. Measurements of the projected equatorial rotation velocity ($v \sin i$) were obtained through individual fits to several small (5 nm) regions between 500 nm and 550 nm, avoiding any inter-order gaps. The final values were determined by calculating the mean and sample deviation of the values obtained in the small spectral regions.

An independent set of $v \sin i$ values were determined for some spectra using the Grid Search in Stellar Parameters (GSSP) software[25]. GSSP is designed to fit a grid of synthetic spectra with varying $T_{\rm eff}$, $\log\ g$, ξ, $v \sin i$ and $[M/H]$ to each observed spectrum and output the χ^2 values of the fit. These synthetic spectra are generated on-the-fly during the fitting process using the SYNTHV radiative transfer code[26] combined with a grid of atmospheric models from the LLMODELS code[27]. We fixed the microturbulent velocity ξ at 2.0 km s^{-1} to prevent degeneracies with metallicity. The derived values were found to be in good agreement with the results from the UCLSYN spectral synthesis.

Table S2 lists the determined $v \sin i$ values for each star. Asterisks (*) indicates close binaries

(see Sec. 2), meaning that $v \sin i$ may not be reliable. We included six stars (below the line) for which we obtained spectroscopy but which are not in Table S1 because their pulsations—while at high frequency— do not show a clear value of $\Delta\nu$.

To determine membership of moving groups, clusters and stellar streams, we calculated barycentric radial velocities using the Python implementation `barycorrPy`[28] of the barycentric correction algorithm of Wright et al. (2014)[29]. These were combined with space motions calculated from *Gaia* DR2 astrometry, and Bayesian posterior probabilities of membership in known nearby moving groups were calculated using `Banyan` Σ[30].

4 Stellar Models

The stellar models presented in Fig. 2 used the 'astero' extension of MESA (Modules for Experiments in Stellar Astrophysics)[31]. We used two approaches that gave similar results. One was based on a model grid calculated with MESA (v8118), where we varied mass (0.80–1.90 $M_\odot$ in steps of 0.01 $M_\odot$) and metallicity ([Fe/H] from -0.5 to 0.5 in steps of 0.1). We used a fixed (solar-calibrated) mixing-length parameter of $\alpha_{\rm MLT}$ = 1.9 and a helium-to-heavy-element enrichment ratio of 1.33. The best-fitting model was found by Maximum Likelihood Estimation, where we included effective temperature, metallicity, luminosity and all identified pulsation frequencies. Equal weight was given in the likelihood function to the following five observables: frequencies of radial modes, frequencies of dipolar modes, effective temperature, metallicity and luminosity. The other approach used the automated simplex search in MESA-astero (v7503), where the fit was guided by the observed radial modes only. The search was allowed to vary the mass, metallicity, mixing length, and the age of the model in order to converge to the best fit. A helium-to-heavy-element enrichment ratio of 1.4 was used. Both approaches assumed a primordial helium abundance of 0.249 and we did not make any correction for surface effects in the way that is commonly done for solar-like stars[32].

For Fig. 3a we used the evolutionary tracks with solar metallicity ($X = 0.71$, $Z = 0.014$) from Murphy et al. (2019)[33]. The other parameters of those tracks are $\alpha_{\rm MLT} = 1.8$, exponential core overshooting of 0.015 H_p (pressure scale heights), exponential H-burning shell over- and undershooting of 0.015 H_p, exponential envelope overshooting of 0.025 H_p, diffusive mixing $\log D_{\rm mix} = 0$ (in cm^{2}s^1), OPAL opacities, and the[34] solar abundance mixture. As noted by Murphy et al. (2019), these tracks are in good agreement with the MIST tracks computed with no rotation and similar metallicities, except that the former have a longer main-sequence phase. This is not expected to be important for our targets, which are mostly young (close to the ZAMS). Although it is possible for δ Scuti pulsations to occur in the pre-main-sequence (PMS) phase, prior to the onset of hydrogen burning[35], there is no indication of a PMS classification for most of the stars in our sample.

5 Additional references and notes on individual stars

As mentioned in the main text, several previous studies have reported regular frequency spacings in the Fourier amplitude spectra of δ Scuti stars[13,36–51]. Among these, the following stars are included in our sample:

- HD 187547 (KIC 7548479): the large frequency spacing was previously reported as 40.5 μHz (3.5 d^{-1})[40,52], which is factor of two smaller than the value we have identified from the same *Kepler* observations.

- HD 34282 (V1366 Ori): based on observations with MOST, Casey et al. (2013)[13] reported a large separation of 3.75 d^{-1}, which is half the value reported here. V1366 Ori is a Herbig Ae star[53], so it may be pre-main sequence. Its classification in SIMBAD as an eclipsing binary appears to incorrect.

- β Pic: known to be a high-frequency δ Scuti star[54,55], but a value for the large separation has not been reported.

The following stars are not in our sample but seem likely to be high-frequency δ Scuti stars with regular spacings:

- HD 144277: based on MOST and CoRoT data, Zwintz et al. (2011)[41] suggested a large separation of 7.2 d^{-1}. This star will not be observed by *TESS* in its nominal two-year mission[56]

- HD 261711: based on MOST and CoRoT data, Zwintz et al. (2013)[42] suggested a large separation of 6.72 d^{-1}. This star was observed by *TESS* in Sector 6, but only in long-cadence mode.

- HD 174966: based on CoRoT data, García Hernández et al. (2013)[44] suggested a large separation of 5.53 d^{-1}. This star will not be observed by *TESS* in its nominal two-year mission[56].

- XX Pyx: based on ground-based multisite observations, Handler et al. (2000)[36] reported 22 pulsation frequencies in the range 27 to 76 d^{-1}, and suggest a large separation of 4.63 d^{-1}. We have examined the published frequencies for this star using échelle diagrams and confirm that a value of $\Delta\nu = 4.70\,d^{-1}$ gives a reasonably good alignment of the peaks. This star will not be observed by *TESS* in its nominal two-year mission[56].

References

1. https://mast.stsci.edu/portal/Mashup/Clients/Mast/Portal.html

2. Høg, E. *et al.* The Tycho-2 catalogue of the 2.5 million brightest stars. *Astron. Astrophys.* **355**, L27–L30 (2000).

3. Bessell, M. S. The Hipparcos and Tycho Photometric System Passbands. *Pub. Astron. Soc. Pac.* **112**, 961–965 (2000).

4. Flower, P. J. Transformations from Theoretical Hertzsprung-Russell Diagrams to Color-Magnitude Diagrams: Effective Temperatures, B-V Colors, and Bolometric Corrections. *Astrophys. J.* **469**, 355 (1996).

5. Lindegren, L. *et al.* Gaia Data Release 2. The astrometric solution. *Astron. Astrophys.* **616**, A2 (2018).

6. Bovy, J., Rix, H.-W., Green, G. M., Schlafly, E. F. & Finkbeiner, D. P. On Galactic Density Modeling in the Presence of Dust Extinction. *Astrophys. J.* **818**, 130 (2016).

7. Huber, D. *et al.* The K2 Ecliptic Plane Input Catalog (EPIC) and Stellar Classifications of 138,600 Targets in Campaigns 1-8. *Astrophys. J.* **224**, 2 (2017).

8. Choi, J. *et al.* Mesa Isochrones and Stellar Tracks (MIST). I. Solar-scaled Models. *Astrophys. J.* **823**, 102 (2016).

9. Casagrande, L. *et al.* New constraints on the chemical evolution of the solar neighbourhood and Galactic disc(s). Improved astrophysical parameters for the Geneva-Copenhagen Survey. *Astron. Astrophys.* **530**, A138 (2011).

10. Huber, D. *et al.* Revised Stellar Properties of Kepler Targets for the Quarter 1-16 Transit Detection Run. *Astrophys. J. Suppl. Ser.* **211**, 2 (2014).

11. Mathur, S. *et al.* Revised Stellar Properties of Kepler Targets for the Q1-17 (DR25) Transit Detection Run. *Astrophys. J. Suppl. Ser.* **229**, 30 (Erratum: ApJS, 234, 43) (2017).

12. Brown, T. M., Latham, D. W., Everett, M. E. & Esquerdo, G. A. Kepler Input Catalog: Photometric Calibration and Stellar Classification. *Astron. J.* **142**, 112 (2011).

13. Casey, M. P. *et al.* MOST observations of the Herbig Ae δ-Scuti star HD 34282. *Mon. Not. R. Astron. Soc.* **428**, 2596–2604 (2013).

14. Mason, B. D., Wycoff, G. L., Hartkopf, W. I., Douglass, G. G. & Worley, C. E. The 2001 US Naval Observatory Double Star CD-ROM. I. The Washington Double Star Catalog. *Astron. J.* **122**, 3466–3471 (2001).

15. Vogt, S. S. *et al.* HIRES: the high-resolution echelle spectrometer on the Keck 10-m Telescope. In Crawford, D. L. & Craine, E. R. (eds.) *Society of Photo-Optical Instrumentation Engineers (SPIE) Conference Series*, vol. 2198 of *Society of Photo-Optical Instrumentation Engineers (SPIE) Conference Series*, 362 (1994).

16. Howard, A. W. *et al.* The California Planet Survey. I. Four New Giant Exoplanets. *Astrophys. J.* **721**, 1467–1481 (2010).

17. Siverd, R. J. *et al.* NRES: the network of robotic echelle spectrographs. In *Ground-based and Airborne Instrumentation for Astronomy VII*, vol. 10702 of *Society of Photo-Optical Instrumentation Engineers (SPIE) Conference Series*, 107026C (2018).

18. Brown, T. M. *et al.* Las Cumbres Observatory Global Telescope Network. *Pub. Astron. Soc. Pac.* **125**, 1031 (2013).

19. Smith, K. C. & Dworetsky, M. M. Report for Workshop on Elemental Abundances Analyses. In Adelman, S. J. & Lanz, T. (eds.) *Elemental Abundance Analyses*, 32 (1988).

20. Smith, K. C. *The chemical compositions of mercury-manganese stars from ultraviolet spectra*. Ph.D. thesis, University of London, University College London (United Kingdom (1992).

21. Castelli, F., Gratton, R. G. & Kurucz, R. L. Notes on the convection in the ATLAS9 model atmospheres. *Astron. Astrophys.* **318**, 841–869 (1997).

22. Kupka, F., Piskunov, N., Ryabchikova, T. A., Stempels, H. C. & Weiss, W. W. VALD-2: Progress of the Vienna Atomic Line Data Base. *Astron. Astrophys. Suppl. Ser.* **138**, 119–133 (1999).

23. Niemczura, E. *et al.* Spectroscopic survey of Kepler stars. I. HERMES/Mercator observations of A- and F-type stars. *Mon. Not. R. Astron. Soc.* **450**, 2764–2783 (2015).

24. Niemczura, E. *et al.* Spectroscopic survey of Kepler stars - II. FIES/NOT observations of A- and F-type stars. *Mon. Not. R. Astron. Soc.* **470**, 2870–2889 (2017).

25. Tkachenko, A. Grid search in stellar parameters: a software for spectrum analysis of single stars and binary systems. *Astron. Astrophys.* **581**, A129 (2015).

26. Tsymbal, V. STARSP: A Software System For the Analysis of the Spectra of Normal Stars. In Adelman, S. J., Kupka, F. & Weiss, W. W. (eds.) *M.A.S.S., Model Atmospheres and Spectrum Synthesis*, vol. 108 of *Astronomical Society of the Pacific Conference Series*, 198 (1996).

27. Shulyak, D., Tsymbal, V., Ryabchikova, T., Stütz, C. & Weiss, W. W. Line-by-line opacity stellar model atmospheres. *Astron. Astrophys.* **428**, 993–1000 (2004).

28. Kanodia, S. & Wright, J. Python leap second management and implementation of precise barycentric correction (barycorrpy). *Research Notes of the AAS* **2**, 4 (2018).

29. Wright, J. T. & Eastman, J. D. Barycentric Corrections at 1 cm s^{-1} for Precise Doppler Velocities. *Pub. Astron. Soc. Pac.* **126**, 838 (2014).

30. Gagné, J. *et al.* BANYAN. XI. The BANYAN Σ Multivariate Bayesian Algorithm to Identify Members of Young Associations with 150 pc. *Astrophys. J.* **856**, 23 (2018).

31. Paxton, B. *et al.* Modules for Experiments in Stellar Astrophysics (MESA): Planets, Oscillations, Rotation, and Massive Stars. *Astrophys. J. Suppl. Ser.* **208**, 4 (2013).

32. Ball, W. H. & Gizon, L. A new correction of stellar oscillation frequencies for near-surface effects. *Astron. Astrophys.* **568**, A123 (2014).

33. Murphy, S. J., Hey, D., Van Reeth, T. & Bedding, T. R. Gaia-derived luminosities of Kepler A/F stars and the pulsator fraction across the δ Scuti instability strip. *Mon. Not. R. Astron. Soc.* **485**, 2380–2400 (2019).

34. Asplund, M., Grevesse, N., Sauval, A. J. & Scott, P. The Chemical Composition of the Sun. *Ann. Rev. Astron. Astrophys.* **47**, 481–522 (2009).

35. Zwintz, K. *et al.* Echography of young stars reveals their evolution. *Science* **345**, 550–553 (2014).

36. Handler, G. *et al.* Delta Scuti Network observations of XX Pyx: detection of 22 pulsation modes and of short-term amplitude and frequency variations. *Mon. Not. R. Astron. Soc.* **318**, 511–525 (2000).

37. García Hernández, A. *et al.* Asteroseismic analysis of the CoRoT δ Scuti star HD 174936. *Astron. Astrophys.* **506**, 79–83 (2009).

38. Breger, M., Lenz, P. & Pamyatnykh, A. A. Towards mode selection in δ Scuti stars: regularities in observed and theoretical frequency spectra. *Mon. Not. R. Astron. Soc.* **396**, 291–298 (2009).

39. Breger, M. *et al.* Regularities in frequency spacings of δ Scuti stars: the Kepler star KIC 9700322. *Mon. Not. R. Astron. Soc.* **414**, 1721–1731 (2011).

40. Antoci, V. *et al.* The excitation of solar-like oscillations in a δSct star by efficient envelope convection. *Nature* **477**, 570–573 (2011).

41. Zwintz, K. *et al.* Regular frequency patterns in the classical δ Scuti star HD 144277 observed by the MOST satellite. *Astron. Astrophys.* **533**, A133 (2011).

42. Zwintz, K. *et al.* Regular frequency patterns in the young δ Scuti star HD 261711 observed by the CoRoT and MOST satellites. *Astron. Astrophys.* **552**, A68 (2013).

43. Paparó, M. *et al.* CoRoT 102749568: mode identification in a δ Scuti star based on regular spacings. *Astron. Astrophys.* **557**, A27 (2013).

44. García Hernández, A. *et al.* An in-depth study of HD 174966 with CoRoT photometry and HARPS spectroscopy. Large separation as a new observable for δ Scuti stars. *Astron. Astrophys.* **559**, A63 (2013).

45. Suárez, J. C. *et al.* Measuring mean densities of δ Scuti stars with asteroseismology. Theoretical properties of large separations using TOUCAN. *Astron. Astrophys.* **563**, A7 (2014).

46. Maceroni, C. *et al.* KIC 3858884: a hybrid δ Scuti pulsator in a highly eccentric eclipsing binary. *Astron. Astrophys.* **563**, A59 (2014).

47. García Hernández, A. *et al.* Observational $\Delta\nu$-ρ Relation for δ Sct Stars using Eclipsing Binaries and Space Photometry. *Astrophys. J.* **811**, L29 (2015).

48. Paparó, M., Benkő, J. M., Hareter, M. & Guzik, J. A. Unexpected Series of Regular Frequency Spacing of δ Scuti Stars in the Non-asymptotic Regime. I. The Methodology. *Astrophys. J.* **822**, 100 (2016).

49. Paparó, M., Benkő, J. M., Hareter, M. & Guzik, J. A. Unexpected Series of Regular Frequency Spacing of δ Scuti Stars in the Non-asymptotic Regime. II. Sample-Echelle Diagrams and Rotation. *The Astrophysical Journal Supplement Series* **224**, 41 (2016).

50. Michel, E. *et al.* What CoRoT tells us about δ Scuti stars. Existence of a regular pattern and seismic indices to characterize stars. In *EPJWC*, vol. 160 of *EPJWC*, 03001 (2017).

51. Bowman, D. M. & Kurtz, D. W. Characterizing the observational properties of δ Sct stars in the era of space photometry from the Kepler mission. *Mon. Not. R. Astron. Soc.* **476**, 3169–3184 (2018).

52. Antoci, V. *et al.* The Role of Turbulent Pressure as a Coherent Pulsational Driving Mechanism: The Case of the δ Scuti Star HD 187547. *Astrophys. J.* **796**, 118 (2014).

53. Mora, A. *et al.* EXPORT: Spectral classification and projected rotational velocities of Vega-type and pre-main sequence stars. *Astron. Astrophys.* **378**, 116–131 (2001).

54. Mékarnia, D. *et al.* The δ Scuti pulsations of β Pictoris as observed by ASTEP from Antarctica. *Astron. Astrophys.* **608**, L6 (2017).

55. Zwintz, K. *et al.* Revisiting the pulsational characteristics of the exoplanet host star β Pictoris. *arXiv e-prints* arXiv:1905.12545 (2019).

56. `https://heasarc.gsfc.nasa.gov/cgi-bin/tess/webtess/wtv.py`

57. Rodríguez, E., López-González, M. J. & López de Coca, P. A revised catalogue of delta Sct stars. *Astron. Astrophys. Suppl. Ser.* **144**, 469–474 (2000).

58. Holdsworth, D. L. *et al.* High-frequency A-type pulsators discovered using SuperWASP. *Mon. Not. R. Astron. Soc.* **439**, 2078–2095 (2014).

59. Gray, R. O. *et al.* The Discovery of λ Bootis Stars: The Southern Survey I. *Astron. J.* **154**, 31 (2017).

60. Murphy, S. J. *et al.* An Evaluation of the Membership Probability of 212 λ Boo Stars. I. A Catalogue. *Pub. Astron. Soc. Aust.* **32**, e036 (2015).

61. Torres, C. A. O. *et al.* Search for associations containing young stars (SACY). I. Sample and searching method. *Astron. Astrophys.* **460**, 695–708 (2006).

62. Zuckerman, B., Rhee, J. H., Song, I. & Bessell, M. S. The Tucana/Horologium, Columba, AB Doradus, and Argus Associations: New Members and Dusty Debris Disks. *Astrophys. J.* **732**, 61 (2011).

63. Mamajek, E. E. & Bell, C. P. M. On the age of the β Pictoris moving group. *Mon. Not. R. Astron. Soc.* **445**, 2169–2180 (2014).

64. Murphy, S. J. & Lawson, W. A. New low-mass members of the Octans stellar association and an updated 30-40 Myr lithium age. *Mon. Not. R. Astron. Soc.* **447**, 1267–1281 (2015).

65. Bell, C. P. M., Mamajek, E. E. & Naylor, T. A self-consistent, absolute isochronal age scale for young moving groups in the solar neighbourhood. *Mon. Not. R. Astron. Soc.* **454**, 593–614 (2015).

66. Meingast, S., Alves, J. & Fürnkranz, V. Extended stellar systems in the solar neighborhood . II. Discovery of a nearby 120 degree stellar stream in Gaia DR2. *Astron. Astrophys.* **622**, L13 (2019).

67. Paunzen, E. *et al.* λ Bootis stars in the SuperWASP survey. *Mon. Not. R. Astron. Soc.* **453**, 1241–1248 (2015).

68. Royer, F., Grenier, S., Baylac, M. O., Gómez, A. E. & Zorec, J. Rotational velocities of A-type stars in the northern hemisphere. II. Measurement of v sin i. *Astron. Astrophys.* **393**, 897–911 (2002).

69. Royer, F., Zorec, J. & Gómez, A. E. Rotational velocities of A-type stars. III. Velocity distributions. *Astron. Astrophys.* **463**, 671–682 (2007).

70. Schröder, C., Reiners, A. & Schmitt, J. H. M. M. Ca II HK emission in rapidly rotating stars. Evidence for an onset of the solar-type dynamo. *Astron. Astrophys.* **493**, 1099–1107 (2009).

Table S1 | Properties of high-frequency δ Scuti stars. An asterisk (*) indicates a close binary (see Sec. 2), meaning that stellar parameters (V, $T_{\rm eff}$, L and ρ) may not be reliable. References indicate classifications as δ Scuti stars [13,40,52,54,55,57,58], λ Boo stars[59,60] and members of young moving groups, clusters or stellar streams[61–66].

TIC	HD	Name	V	$T_{\rm eff}$ (K)	$L/L_\odot$	$\rho/\rho_\odot$	$\Delta\nu$ (d^{-1})	ϵ	Refs.
589826	30422	EX Eri	6.18	7939	$8.42^{+0.08}_{-0.08}$	$0.40^{+0.06}_{-0.03}$	6.52	1.86	57,60
9147509*	25369		9.68	—-	—	—	6.15	1.65	
11199304	290750		9.77	9171	$19.14^{+0.82}_{-0.78}$	$0.35^{+0.04}_{-0.04}$	5.96	1.49	
11361473	290799	V1790 Ori	10.67	8783	$13.21^{+0.82}_{-0.76}$	$0.42^{+0.05}_{-0.05}$	7.55	1.65	60,67
24344701	34282	V1366 Ori	9.92	—	—	—	7.40	1.71	13
31475829	37286	HR 1915	6.26	8077	$8.18^{+0.09}_{-0.09}$	$0.47^{+0.03}_{-0.05}$	7.30	—	62,68
32763133	38629		8.92	8166	$11.27^{+0.28}_{-0.27}$	$0.35^{+0.04}_{-0.04}$	7.35	1.77	58
34197596	25674		8.69	8261	$10.20^{+0.28}_{-0.27}$	$0.42^{+0.04}_{-0.04}$	6.75	1.79	58
34737955	44930		9.42	7317	$7.17^{+0.27}_{-0.26}$	$0.33^{+0.05}_{-0.04}$	6.03	1.67	59
37498433	42608		9.85	8171	$10.05^{+0.28}_{-0.27}$	$0.40^{+0.05}_{-0.05}$	7.10	1.57	58,61,64
43363194	3622		7.77	7928	$7.86^{+0.15}_{-0.15}$	$0.45^{+0.05}_{-0.04}$	6.89	1.61	
44645679	24975		7.24	7794	$9.20^{+0.11}_{-0.11}$	$0.37^{+0.01}_{-0.04}$	6.23	1.58	
71134596	28548		9.22	8512	$10.82^{+0.33}_{-0.32}$	$0.46^{+0.05}_{-0.05}$	7.50	1.67	58,59
78492107	50153		7.03	7824	$9.15^{+0.11}_{-0.11}$	$0.37^{+0.03}_{-0.04}$	6.85	1.60	
100531058	38597		8.65	8425	$10.38^{+0.20}_{-0.20}$	$0.44^{+0.03}_{-0.05}$	6.90	1.68	58
112484997	59594	V349 Pup	7.32	7798	$8.06^{+0.09}_{-0.09}$	$0.39^{+0.05}_{-0.04}$	6.65	1.61	57
117766204	45424		7.18	8062	$10.39^{+0.15}_{-0.15}$	$0.36^{+0.04}_{-0.04}$	6.54	1.86	
122615966	17341		9.32	7810	$10.05^{+0.29}_{-0.28}$	$0.32^{+0.04}_{-0.04}$	5.90	1.73	59
122686610	17693		7.80	7879	$10.21^{+0.15}_{-0.15}$	$0.33^{+0.04}_{-0.04}$	6.41	1.61	
124381332		TYC 5945-497-1	9.69	8271	$10.02^{+0.34}_{-0.33}$	$0.42^{+0.05}_{-0.05}$	7.45	1.61	58
124429243	42915		9.04	8516	$12.82^{+0.44}_{-0.42}$	$0.38^{+0.04}_{-0.04}$	6.40	1.98	58,61,64
143381070		SAO 150524	9.46	8028	$7.88^{+0.22}_{-0.21}$	$0.48^{+0.05}_{-0.05}$	7.63	—	
148228220	48985		9.04	7709	$11.60^{+0.27}_{-0.27}$	$0.25^{+0.03}_{-0.03}$	7.25	1.56	
150272131	44726		10.38	7885	$7.87^{+0.20}_{-0.20}$	$0.45^{+0.05}_{-0.06}$	7.25	1.70	58
159895674	20232		6.88	8058	$8.64^{+0.09}_{-0.09}$	$0.44^{+0.03}_{-0.05}$	6.86	1.64	
172193026	46722		9.29	7812	$8.28^{+0.22}_{-0.21}$	$0.39^{+0.04}_{-0.04}$	6.45	1.71	59
176400189*	75040		9.05	—	—	—	6.64	1.58	
224284988	223011		6.32	7827	$10.49^{+0.13}_{-0.13}$	$0.31^{+0.06}_{-0.04}$	5.93	1.68	
229139161	10779		8.78	7733	$8.13^{+0.15}_{-0.15}$	$0.38^{+0.04}_{-0.04}$	6.80	1.63	
231014033*	10961		9.39	7434	—	—	7.30	1.70	
242944780	24572		9.45	7410	$7.25^{+0.21}_{-0.20}$	$0.34^{+0.05}_{-0.04}$	7.20	1.58	58

TIC	HD	Name	V	$T_{\rm eff}$ (K)	$L/L_\odot$	$\rho/\rho_\odot$	$\Delta\nu$ (d^{-1})	ϵ	Refs.
246902545	31322		9.28	8259	$13.19^{+0.39}_{-0.38}$	$0.32^{+0.04}_{-0.04}$	6.10	1.69	58
255548143	44958	V435 Car	6.74	7655	$7.82^{+0.08}_{-0.08}$	$0.40^{+0.05}_{-0.06}$	6.90	1.58	57
259675399	31640		8.06	7687	$8.25^{+0.12}_{-0.12}$	$0.37^{+0.04}_{-0.04}$	6.41	1.75	
260161111		TYC 8533-329-1	10.70	8368	$9.33^{+0.34}_{-0.33}$	$0.48^{+0.06}_{-0.05}$	7.27	—	58
269792989*	29783		7.87	—	—	—	6.74	1.79	61, 64
270577175	39060	β Pic	3.85	8082	$8.49^{+0.19}_{-0.18}$	$0.45^{+0.04}_{-0.05}$	6.95	—	54, 55, 63
274038922	20203		8.85	7973	$8.06^{+0.20}_{-0.20}$	$0.45^{+0.05}_{-0.05}$	7.20	1.76	58
278179191	59104		8.50	7364	$6.15^{+0.09}_{-0.09}$	$0.39^{+0.06}_{-0.04}$	6.96	1.67	
281499618	2280		9.13	7506	$5.52^{+0.13}_{-0.13}$	$0.50^{+0.05}_{-0.05}$	7.17	1.73	
282265535	40317		8.45	8698	$10.58^{+0.34}_{-0.33}$	$0.51^{+0.06}_{-0.05}$	6.95	1.63	
284348793	54711		9.01	8195	$9.22^{+0.25}_{-0.25}$	$0.44^{+0.06}_{-0.05}$	7.08	1.65	
287347434	99506		8.36	7972	$7.58^{+0.20}_{-0.20}$	$0.48^{+0.06}_{-0.05}$	7.05	1.59	
294157254	55863		9.06	7645	$7.80^{+0.22}_{-0.21}$	$0.38^{+0.05}_{-0.05}$	6.92	1.57	
306773428*	67688		7.66	—	—	—	7.04	1.59	
316806320*	222496		9.48	—	—	—	5.63	1.71	
316920092	31901		9.07	7768	$7.74^{+0.23}_{-0.23}$	$0.42^{+0.05}_{-0.05}$	6.97	1.56	66
327996759*	220811		6.91	—	—	—	6.04	1.82	
332516661	78198		9.50	7341	$7.79^{+0.27}_{-0.26}$	$0.31^{+0.04}_{-0.04}$	5.90	1.65	
340358522		TYC 8564-537-1	10.59	7493	$7.30^{+0.21}_{-0.20}$	$0.36^{+0.05}_{-0.04}$	7.15	1.54	
348792358	32433		9.22	7696	$7.32^{+0.18}_{-0.18}$	$0.42^{+0.04}_{-0.05}$	6.95	1.54	
349645354		SAO 249859	9.79	7066	$7.99^{+0.20}_{-0.19}$	$0.23^{+0.04}_{-0.03}$	5.34	1.69	
388351327*	70510		6.75	—	—	—	7.16	1.68	
408906554	42005		9.54	8031	$8.75^{+0.23}_{-0.22}$	$0.42^{+0.04}_{-0.05}$	7.16	1.57	58
431695696		TYC 85-867-1	9.63	7961	$8.85^{+0.44}_{-0.41}$	$0.41^{+0.05}_{-0.05}$	7.26	1.61	
459942890*	25248		8.60	—	—	—	7.16	1.55	
463556278*	89263	HR 4043	6.22	—	—	—	7.02	1.71	65
KIC 7548479	187547		8.40	7474	$6.74^{+0.10}_{-0.10}$	$0.40^{+0.07}_{-0.05}$	7.00	1.61	40, 52
KIC 8415752		TYC 3132-1272-1	10.67	7777	$9.83^{+0.33}_{-0.32}$	$0.32^{+0.04}_{-0.04}$	6.20	1.63	
KIC 9450940			12.68	7922	$8.59^{+0.47}_{-0.44}$	$0.41^{+0.05}_{-0.06}$	6.15	1.67	

Table S2 | Projected rotational velocities from high-resolution spectroscopy. An asterisk (*) indicates a close binary (see Sec. 2), meaning that $v \sin i$ may not be reliable. Stars below the line are not part of the sample listed in Table S1 that have clear values of $\Delta\nu$.

TIC	HD	Name	$v \sin i$ (km s^{-1})	source
589826	30422	EX Eri	128	literature[69]
24344701	34282	V1366 Ori	129 ± 11	literature[53]
31475829	37286	HR 1915	70	literature[68]
37498433	42608		41 ± 1	Keck
43363194	3622		50 ± 6	LCO
124381332		TYC 5945-497-1	178 ± 37	Keck
124429243	42915		118 ± 5	Keck
176400189*	75040		24 ± 3	Keck
224284988	223011		43 ± 2	LCO
255548143	44958	V435 Car	114 ± 11	LCO
270577175	39060	β Pic	122	literature[70]
287347434	99506		26 ± 2	Keck
327996759*	220811		261 ± 40	Keck & LCO
332516661	78198		45 ± 1	Keck
388351327*	70510		94 ± 10	LCO
463556278*	89263	HR 4043	100 ± 7	Keck
KIC 7548479	187547		10 ± 2	literature[40]
KIC 8415752		TYC 3132-1272-1	18 ± 1	Keck
KIC 9450940			10 ± 1	Keck
4351100	294060		79 ± 3	Keck
48657402*		TYC 6515-7-1	42 ± 2	Keck
92734713	200835		244 ± 45	Keck
248439776	293856		109 ± 6	Keck
248990523		TYC 4759-318-1	118 ± 5	Keck
440736236	55463		164 ± 25	Keck

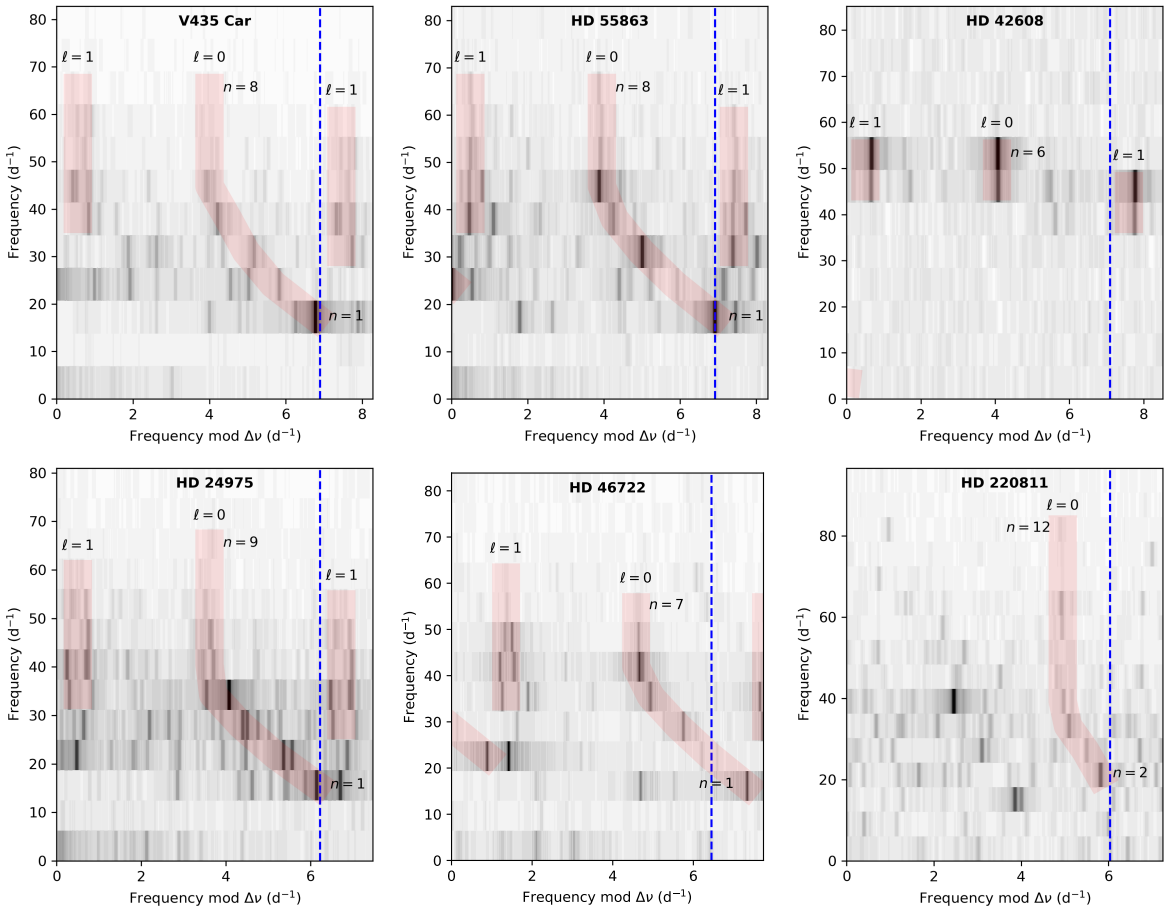

Figure S1 | **More examples of mode identifications in δ Scuti stars.** The amplitude spectra are shown in échelle format, with segments of equal length being stacked vertically. The vertical dashed line shows the value of $\Delta\nu$ used in each case, with a repeated overlap region added on the right for clarity. The greyscale shows the observed amplitude spectrum of data from the *TESS* spacecraft, where the number of 27-day sectors was four for V435 Car, three for HD 55863, two for HD 24975 and HD 46722, and one for HD 42608 and HD 220811. Smoothing was applied to the observed amplitude spectra before plotting and the red stripes mark overtones sequences of $l = 0$ and $l = 1$ modes.

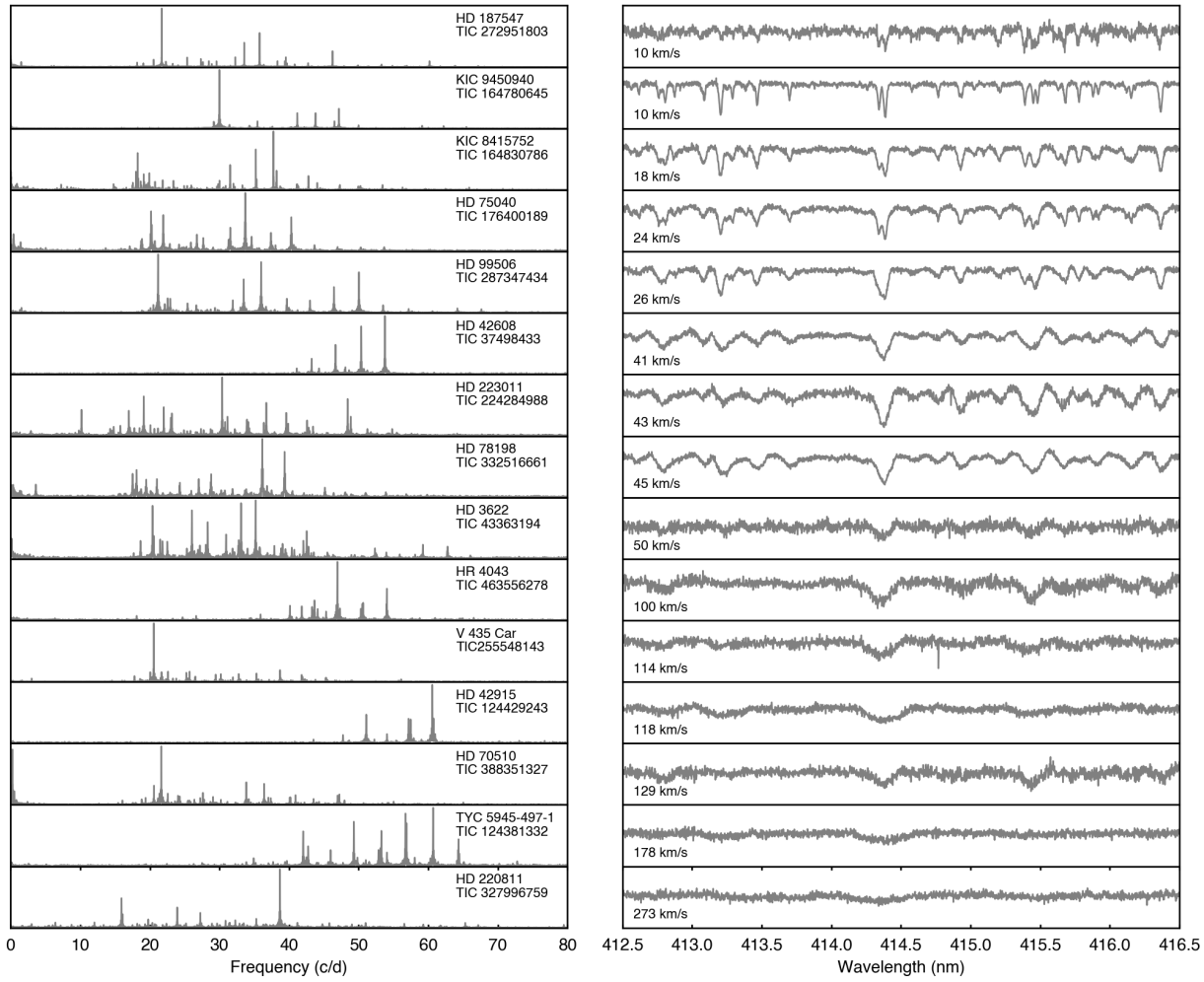

Figure S2 | Fourier amplitude spectra and high-resolution spectra of high-frequency δ Scuti stars. Measured $v \sin i$ values are shown in the right panel and the stars are sorted by increasing $v \sin i$.